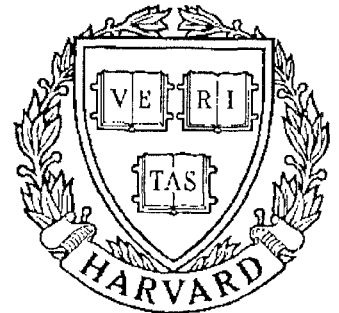


TECHNICAL RESEARCH REPORT



S Y S T E M S
R E S E A R C H
C E N T E R



*Supported by the
National Science Foundation
Engineering Research Center
Program (NSFD CD 8803012),
Industry and the University*

Kinematic Synthesis of Tendon-Driven Manipulators with Isotropic Transmission Characteristics

by Y-J. Ou and L-W. Tsai

KINEMATIC SYNTHESIS OF TENDON-DRIVEN MANIPULATORS WITH ISOTROPIC TRANSMISSION CHARACTERISTICS

Yeong-Jeong Ou
Graduate Research Assistant

Lung-Wen Tsai
Professor
Fellow ASME

Mechanical Engineering Department
and
Institute for Systems Research
University of Maryland
College Park, MD 20742

November 17, 1992

ABSTRACT

This paper presents a methodology for kinematic synthesis of tendon-driven manipulators with isotropic transmission characteristics. The force transmission characteristics, from the end-effector space to the actuator space, has been investigated. It is shown that tendon forces required to act against externally applied forces are functions of the structure matrix, its null vector, and the manipulator Jacobian matrix. Design equations for synthesizing a manipulator to possess isotropic transmission characteristics are derived. An isotropic transmission is defined as one for which the product of the structure matrix and Jacobian matrix has a unity condition number, and the direction of the null vector points in the $[1, 1, \dots, 1]^T$ direction. Two examples are used to demonstrate the methodology. It is shown that manipulators which possess isotropic transmission characteristics do have much better force distribution among their tendons.

INTRODUCTION

The advantage of using tendons for transmitting power in robot manipulators is that it permits actuators to be installed on or somewhere close to the fixed frame. Thus, the size and inertia of the manipulating system can be reduced. Several tendon-driven manipulators can be found in the literature. Okada (1977) used endless type tendons (belts) in the design of the transmission system of a three fingered hand. Though only n actuators are needed to actuate an n -dof manipulator, pretension is required to prevent belts from slacking. For high speed operations, pretension causes

an excessive amount of friction and, therefore, degrades the efficiency of the transmission system. Rovetta (1977) and, Sugano and Kato (1987) developed similar transmission devices using springs for pretension of tendons.

To avoid high pretension, Jacobsen, et al. (1985) used two tendons (two actuators), antagonistically pulled against each other, to drive each joint of the Utah/MIT dexterous hand. The device inevitably increases the numbers of tendons, actuators, pulleys, and the complexity of controllers. On the other hand, Morecki, et al. (1980) employed seven tendons to actuate a six-dof manipulator. They showed that $n + 1$ is the minimum number of tendons required to achieve full control of an n -dof manipulator. Salisbury (1982) designed a three-fingered Stanford/JPL hand in which each finger has three degrees of freedom, and is actuated by four tendons. Both Morecki and Salisbury's designs require no pretension and, therefore, result in lower tendon forces. The number of actuators needed outnumber that used in belt driven devices by one only.

In order to better design tendon-driven manipulators, Lee and Tsai (1991) developed a methodology for the synthesis of kinematic structures with pseudo-triangular structure matrices. However, they only focused on those types of structures in which pulleys mounted on one common joint axis are all of the same size. In this study, we allow the pulleys to assume different sizes, and seek for the design equations for synthesizing manipulators with isotropic transmission characteristics.

The condition number is known as a measure of error-amplifying factor in a linear transformation system. For a manipulator system, it refers to the amplification of error from the actuator space to the end-effector space.

A point in the workspace of a manipulator where the condition number is equal to one is called an isotropic point. At an isotropic point, output error in the end-effector space due to input error in the actuator space has a minimum upper bound. The property of kinematic isotropy is, therefore, very important in achieving accurate control of robot manipulators.

Many researchers defined the condition number as the ratio of the maximal singular value to the minimal singular value of the Jacobian matrix \mathbf{J} (Salisbury and Craig, 1982; Yoshikawa, 1984; Asada, et al., 1985; Gosselin and Angeles, 1988). The Jacobian matrix is the matrix which transforms the joint rates into the end-effector velocity. The transformation between the end-effector space and the joint space is said to be isotropic, if the condition number of the Jacobian matrix is equal to one. This definition of isotropic transformation does not take the effect of transmission mechanisms into consideration. Strictly speaking, it is only valid for direct-drive manipulators.

Lee (1991) defined the condition number of a tendon transmission structure as the ratio of the maximal singular value to the minimal singular value of the structure matrix. The structure matrix is the matrix which transforms the joint angles into tendon/actuator displacements. The transformation between the joint space and the actuator/tendon space is said to be isotropic, if the condition number of the structure matrix is equal to one. When the condition number of the Jacobian matrix and that of the structure matrix are both equal to one, an isotropic transformation is obtained for the overall system.

The above two approaches can only achieve partial or limited results. To make the theory complete, Chen and Tsai (1992) first introduced the concept of overall transformation matrix between the actuator space and the end-effector space for gear-coupled manipulators. They defined the isotropic transformation as one which has the unity condition number for the overall transformation matrix. It does not require both the condition numbers of the Jacobian matrix and the structure matrix to be equal to one. Therefore, it gives more flexibility for the synthesis of manipulators. However, their results are not directly applicable to tendon-driven manipulators.

In this paper, we study the overall transformation between the actuator space and the end-effector space of tendon-driven manipulators. First, the necessary conditions for a manipulator to possess isotropic transmission characteristics will be derived. Then, the results will be applied to those types of tendon-driven manipulators with pseudo-triangular structure matrices. Finally, it will be shown that isotropic transmission structures of the general form can be derived from that of the pseudo-triangular form. Two design examples will be used to demonstrate the effects on their performance.

ADMISSIBLE TRANSMISSION STRUCTURES

Figure 1 shows the planar schematic of a general n -dof tendon-driven manipulator with m tendons. See Lee and Tsai (1991) for the definition of the planar representation of a spatial mechanism. The relationship between tendon/actuator displacements and joint angles for such a tendon-driven

manipulator can be expressed as (Lee and Tsai, 1991)

$$\underline{S} = \mathbf{A} \underline{\theta} \quad (1)$$

Similarly, the relationship between tendon forces and joint torques can be expressed as

$$\underline{\tau} = \mathbf{A}^T \underline{\xi} \quad (2)$$

where $\underline{S} = [S_1, S_2, \dots, S_m]^T$ denotes an $m \times 1$ linear displacement vector for the m tendons, $\underline{\theta} = [\theta_1, \theta_2, \dots, \theta_n]^T$ denotes an $n \times 1$ joint angular displacement vector, $\underline{\tau} = [\tau_1, \tau_2, \dots, \tau_n]^T$ denotes an $n \times 1$ joint torque vector, $\underline{\xi} = [\xi_1, \xi_2, \dots, \xi_m]^T$ denotes an $m \times 1$ tendon force vector, and $\mathbf{A} = [a_{ij}]$ is an $m \times n$ structure matrix. Note that the links and joints are numbered sequentially from the distal end of the manipulator as shown in Fig. 1 for the convenience of matrix operations. The absolute value of a_{ij} is equal to the radius of the pulley mounted on the j th joint and routed by the i th tendon. And the sign of a_{ij} is positive if a positive displacement of tendon i produces a positive rotation of the pulley mounted on joint j , otherwise it is negative. The value of a_{ij} is equal to zero if tendon i is not routed about joint j . Figure 2 shows the definition of a_{ij} where the positive axis of rotation points out of the paper.

As pointed out by early researchers (Morecki, et al., 1980; Salisbury and Craig, 1982), a minimum of $n + 1$ tendons is necessary for the control of an n -dof manipulator. Since using more than $n + 1$ tendons would result in more complex transmission structure, it is appropriate to keep the number of tendons to the minimum. In what follows, we shall focus only on those transmission structures which use the minimum number of tendons, that is, $(n + 1) \times n$ transmission structure matrices. A feasible $(n + 1) \times n$ transmission

structure matrix has to satisfy the following conditions (Morecki, et al., 1980; Lee and Tsai, 1991)

- C1. The rank of matrix \mathbf{A} must be equal to n .
- C2. Each element in the null vector of \mathbf{A}^T must be of the same sign and not equal to zero.
- C3. Tendons must be routed from joint to joint in a continuous manner, i.e. non-zero elements in each column of \mathbf{A}^T must be consecutive.

Conditions C1 and C2 ensure all tendons can maintain positive tensions, and condition C3 results from the physical limitation of tendon routing in an articulated mechanism.

Equation (2) transforms tendon forces into joint torques. Given a set of tendon forces, the resultant joint torques are uniquely determined. However, the determination of tendon forces to achieve a set of desired joint torques is an indeterminant problem. From conditions C1 and C2, the inverse transformation of eq. (2) can be written as:

$$\underline{\xi} = \mathbf{A}^{+T} \underline{\tau} + \lambda \underline{\xi}_h \quad (3)$$

where \mathbf{A}^{+T} is the pseudoinverse of \mathbf{A}^T (Ben-Israel and Greville, 1974; Strang, 1980), $\underline{\xi}_h$ is a one-dimensional null vector of \mathbf{A}^T , and λ is an arbitrary constant.

The first term in eq. (3) is known as the particular solution, and the second term is called the homogeneous solution. The homogeneous solution

or the null vector satisfies

$$\mathbf{A}^T \cdot \underline{\xi}_h = 0 \quad (4)$$

Condition C2 can be interpreted as requiring all elements of $\underline{\xi}_h$ to be positive. Using Cramer's rule, the null vector can be written as

$$\underline{\xi}_h = \left[-d_1, d_2, \dots, (-1)^i d_i, \dots, (-1)^{n+1} d_{n+1} \right]^T \quad (5)$$

where d_i is the determinant of the matrix formed by deleting the i th column of \mathbf{A}^T . Since $d_i \neq 0$, for $i = 1, \dots, n+1$, implies that matrix \mathbf{A} is of rank n , conditions C1 and C2 can be combined into a single condition as

$$(-1)^i d_i > 0, \text{ for } i = 1, \dots, n+1 \quad (6)$$

Using eq. (6) and condition C3 as the constraints, all admissible tendon routings can be enumerated. Note that we have allowed pulleys to assume different sizes in this study. Since Lee and Tsai (1991) assumed that all pulleys mounted on the same joint axis are of the same size, their result is a subset of what can be enumerated by using condition C3 and eq. (6).

ISOTROPIC TRANSMISSION STRUCTURES

In this section, necessary and sufficient conditions for a tendon-driven manipulator to possess isotropic transmission characteristics will be derived. We shall assume that dimensions of the links such as the offset distances and twist angles of a manipulator are known. Thus, once the posture of a manipulator is specified, the Jacobian matrix is completely known. Our objective is to find appropriate tendon routings and pulley sizes which

yield isotropic transmission characteristics for the manipulator at a specified posture.

Unity Condition Number

The kinematic relationship between external forces acting on the end-effector and the resultant joint torques can be written as

$$\underline{\tau} = \mathbf{J}^T \underline{f} \quad (7)$$

where \mathbf{J}^T is the transpose of the $n \times n$ Jacobian matrix and \underline{f} is an $n \times 1$ general force vector acting on the end-effector.

Substituting eq. (7) into (3), we obtain the force relation between the tendon space and the end-effector space as

$$\underline{\xi} = \mathbf{A}^{+T} \mathbf{J}^T \underline{f} + \lambda \underline{\xi}_h \quad (8)$$

From eq. (8), we see that tendon forces can be decomposed into two mutually perpendicular components: the homogeneous solution $\underline{\xi}_h$ and the particular solution $\underline{\xi}_p = \mathbf{A}^{+T} \mathbf{J}^T \underline{f}$. The homogeneous solution has no effect on the resultant joint torques, while the particular solution depends on the externally applied forces, and the product of the matrices \mathbf{A}^{+T} and \mathbf{J}^T . Thus, for tendon-driven manipulators, both the homogeneous solution $\underline{\xi}_h$ and the matrix product $\mathbf{A}^{+T} \mathbf{J}^T$ play important roles in tendon force distribution.

In this paper, we define the condition number as the ratio of the maximal singular value to the minimal singular value of $\mathbf{A}^{+T} \mathbf{J}^T$. When the condition number is equal to one, the columns of $\mathbf{A}^{+T} \mathbf{J}^T$ are orthogonal,

that is (Strang, 1980),

$$\mathbf{J}\mathbf{A}^+\mathbf{A}^{+T}\mathbf{J}^T = \mu^2\mathbf{I}_n \quad (9)$$

where μ is an arbitrary constant and \mathbf{I}_n is the $n \times n$ identity matrix. Using $\mathbf{A}^+ = (\mathbf{A}^T\mathbf{A})^{-1}\mathbf{A}^T$ and $(\mathbf{A}^T\mathbf{A})^{-T} = (\mathbf{A}^T\mathbf{A})^{-1}$, eq. (9) can be simplified as

$$\mathbf{J}(\mathbf{A}^T\mathbf{A})^{-1}\mathbf{A}^T\mathbf{A}(\mathbf{A}^T\mathbf{A})^{-1}\mathbf{J}^T = \mu^2\mathbf{I}_n \quad (10)$$

or

$$\mathbf{J}(\mathbf{A}^T\mathbf{A})^{-1}\mathbf{J}^T = \mu^2\mathbf{I}_n \quad (11)$$

Pre-multiplying \mathbf{J}^T to both sides of eq. (11), we obtain

$$\mathbf{J}^T\mathbf{J}(\mathbf{A}^T\mathbf{A})^{-1}\mathbf{J}^T = \mu^2\mathbf{J}^T \quad (12)$$

Since eq. (12) is valid for any matrix \mathbf{J}^T , we conclude that

$$\mathbf{J}^T\mathbf{J}(\mathbf{A}^T\mathbf{A})^{-1} = \mu^2\mathbf{I}_n \quad (13)$$

Post-multiplying eq. (13) by $(\mathbf{A}^T\mathbf{A})$, we obtain

$$\mathbf{A}^T\mathbf{A} = \frac{1}{\mu^2}\mathbf{J}^T\mathbf{J} \quad (14)$$

Equation (14) is the necessary and sufficient condition for the condition number of $\mathbf{A}^{+T}\mathbf{J}^T$ to be equal to one. Since \mathbf{A} is a matrix of rank n , eq. (14) can only be satisfied at those positions where the Jacobian matrix \mathbf{J} is of rank n . Since the Jacobian matrix is position dependent, the condition number is also position dependent. Therefore, the unity condition number can be achieved only at a specified manipulator posture.

Isotropic Vector

The homogeneous solution, $\underline{\xi}_h$, when multiplied by λ , allows us to adjust tendon forces such that positive tensions can be maintained in all tendons (Salisbury, 1982; Lee and Tsai, 1991). Hence, the direction of the null vector has a significant effect on the distribution of tendon forces. It is highly desirable to have the tendons routed in such a way that its homogeneous solution points in the $[1, 1, \dots, 1]^T$ direction. We call vector $[1, 1, \dots, 1]^T$ the isotropic vector. For the null vector of \mathbf{A}^T to be pointing in the isotropic direction, the following condition must be satisfied.

$$\mathbf{A}^T \cdot [1, 1, \dots, 1]^T = \underline{0} \quad (15)$$

Isotropic Transmission

A manipulator is said to possess isotropic transmission characteristics if its overall transform matrix $\mathbf{A}^{+T}\mathbf{J}^T$ has a unity condition number and if the null vector of \mathbf{A}^T points in the isotropic direction.

Equation (14) assures that \mathbf{A} is a matrix of rank n and eq. (15) indicates that the null vector points in the isotropic direction. We call a structure matrix which satisfies eqs. (14), (15), and condition C3 an isotropic transmission structure. Equation (14) contains $n(n+1)/2$ quadratic equations while eq. (15) contains n linear equations as functions of the matrix elements, a_{ij} . Thus, there are a total of $n(n+3)/2$ equations of constraint imposed on the elements of matrix \mathbf{A} . It turns out that the number of constraint equations is equal to the minimum number of pulleys needed for the routing of an n -dof manipulator with $n+1$ tendons.

Since eq. (14) contains an arbitrary constant μ , we conclude that once a kinematically isotropic transmission arrangement is found, the pulley sizes can be proportionally increased (or decreased) without affecting its isotropic transmission characteristics. The proportional constant, however, does have an effect on the pulley sizes and, therefore, on the resulting tensions in tendons.

In what follows, we will apply eqs. (14) and (15) to the structure synthesis of tendon-driven manipulators. Two types of structure matrices will be studied. The first is that of pseudo-triangular form and the second is of the general form.

MANIPULATORS WITH PSEUDO-TRIANGULAR STRUCTURE MATRICES

For an n -dof tendon-driven manipulator constructed with the minimum number of tendons and pulleys, the structure matrix can be arranged in a pseudo-triangular form as shown below: (Morecki, et al., 1980):

$$\mathbf{A}^T = \begin{bmatrix} a_{11} & a_{21} & 0 & \cdots & \cdots & 0 \\ a_{12} & a_{22} & a_{32} & 0 & \cdots & 0 \\ & \vdots & & & \ddots & \vdots \\ a_{1,n-1} & a_{2,n-1} & \cdots & \cdots & a_{n,n-1} & 0 \\ a_{1,n} & a_{2,n} & \cdots & \cdots & a_{n,n} & a_{n+1,n} \end{bmatrix} \quad (16)$$

where $a_{ij} \neq 0$.

In what follows, we shall identify those pseudo-triangular structure matrices which satisfy eqs. (14) and (15). First, we will investigate a special manipulator whose Jacobian matrix has a unity condition number at a specific posture. For this special manipulator to possess isotropic transmission, the condition number of its structure matrix is also equal to one. Thus, both condition numbers of \mathbf{A}^T and \mathbf{J} are equal to one at the given posture. We will show that there exists only one such structure matrix. Then, we will investigate the case of a general manipulator for which the condition number of its Jacobian matrix is not necessarily equal to one, and show that the structure matrix for such a manipulator can be derived from that of the special manipulator.

Special Manipulator

We first consider a particular manipulator for which the condition number of its Jacobian matrix is equal to one at a specific manipulator posture, that is

$$\mathbf{J}^T \mathbf{J} = c^2 \mathbf{I}_n \quad (17)$$

where c is an arbitrary constant. We seek for the conditions which lead to isotropic transmission at this given posture.

Substituting eq. (17) into (14), yields

$$\mathbf{A}^T \mathbf{A} = \kappa^2 \mathbf{I}_n \quad (18)$$

where $\kappa = c/\mu$.

Expanding eq. (18), we obtain

$$a_{11}^2 + a_{21}^2 = \kappa^2 \quad (19.a)$$

$$a_{11}a_{12} + a_{21}a_{22} = 0 \quad (19.b)$$

$$a_{11}a_{13} + a_{21}a_{23} = 0 \quad (19.c)$$

$$a_{12}^2 + a_{22}^2 + a_{32}^2 = \kappa^2 \quad (19.d)$$

$$a_{12}a_{13} + a_{22}a_{23} + a_{32}a_{33} = 0 \quad (19.e)$$

$$a_{13}^2 + a_{23}^2 + a_{33}^2 + a_{43}^2 = \kappa^2 \quad (19.f)$$

etc.

Substituting eq. (16) into (15), yields

$$a_{11} + a_{21} = 0 \quad (20.a)$$

$$a_{12} + a_{22} + a_{32} = 0 \quad (20.b)$$

$$a_{13} + a_{23} + a_{33} + a_{43} = 0 \quad (20.c)$$

etc.

Solving eqs. (19.a) and (20.a), yields

$$a_{11} = \pm \frac{\kappa}{\sqrt{2}} \quad (21)$$

and

$$a_{21} = \mp \frac{\kappa}{\sqrt{2}} \quad (22)$$

Substituting eqs. (21) and (22) into eq. (19.b), yields

$$a_{12} = a_{22} \quad (23)$$

Substituting eq. (23) into eqs. (19.d) and (20.b) and solving the resulting equations for a_{12} , a_{22} and a_{32} , yields

$$a_{12} = a_{22} = \pm \frac{\kappa}{\sqrt{6}} \quad (24)$$

$$a_{32} = \mp \frac{2\kappa}{\sqrt{6}} \quad (25)$$

Following the same procedure, all the other variables in matrix (16) can be found. After factoring out the common factor, $\kappa/\sqrt{2}$, and letting the first column of the matrix \mathbf{A}^T to assume the positive sign without losing generality (see Lee and Tsai, 1991), we obtain

$$\mathbf{A}^T = \frac{\kappa}{\sqrt{2}} \begin{bmatrix} 1 & -1 & 0 & \cdots & \cdots & 0 \\ 1/\sqrt{3} & 1/\sqrt{3} & -2/\sqrt{3} & 0 & \cdots & 0 \\ 1/\sqrt{6} & 1/\sqrt{6} & 1/\sqrt{6} & -3/\sqrt{6} & 0 \cdots & 0 \\ \cdots & \cdots & \cdots & \cdots & \cdots & \cdots \\ \sqrt{\frac{2}{(n^2+n)}} & \cdots & \cdots & \cdots & \sqrt{\frac{2}{(n^2+n)}} & -\sqrt{\frac{2n^2}{(n^2+n)}} \end{bmatrix} \quad (26)$$

Note that there are $2^n - 1$ isomorphic structure matrices (Lee, 1991) which can be formed by multiplying “-1” to any row or combination of rows of matrix \mathbf{A}^T in eq. (26). The structure matrix shown in eq. (26) satisfies condition C3 automatically. Therefore, if we choose the design position at the special posture where the condition number of the Jacobian matrix is equal to one, eq. (26) is the only admissible pseudo-triangular structure matrix

which yields isotropic transmission characteristics. For this special case, the condition number of \mathbf{A}^T is also equal to one. Hence, the condition number of $\mathbf{A}^{+T}\mathbf{J}^T$ varies as that of \mathbf{J}^T as the end-effector moves away from the design position.

From eq. (26), we see that, starting from the n th joint, the pulleys in each transmission line (each column) become progressive larger as they move away from the base. This is due to the fact that the number of tendons routed over a distal joint is fewer than that routed over a proximal joint. To generate equal amount of joint torque with equal tendon force, pulleys mounted at a distal joint must be larger than that mounted at a proximal joint.

The κ in matrix (26) represents a global amplification factor for sizing the pulleys. The value of κ doesn't change the condition number nor the ratios of tendon forces, however it does have the effect on the magnitude of tendon forces.

General Manipulator

We now consider a general manipulator for which the condition number of its Jacobian matrix \mathbf{J} may not be equal to one anywhere within its workspace. The desired structure matrix can be derived as follows.

Let \mathbf{A} be a pseudo-triangular structure matrix which satisfies eqs. (14) and (15); then \mathbf{A} has independent columns. Using QR factorization, we can express \mathbf{A} as

$$\mathbf{A} = \tilde{\mathbf{Q}}\tilde{\mathbf{R}} \quad (27)$$

where $\tilde{\mathbf{Q}}$ is an $(n + 1) \times n$ real unitary matrix having the form of an upper

pseudo-triangular matrix and $\tilde{\mathbf{R}}$ is an $n \times n$ invertible upper-triangular matrix with positive diagonal entries so that the factorization is unique (Golub and Van Loan, 1983). Since \mathbf{A} satisfies eq. (14), we can write

$$\mathbf{A}^T \mathbf{A} = \frac{1}{\mu^2} \mathbf{J}^T \mathbf{J} \quad (28)$$

Substituting eq. (27) into eq. (28), yields

$$\tilde{\mathbf{R}}^T \tilde{\mathbf{Q}}^T \tilde{\mathbf{Q}} \tilde{\mathbf{R}} = \frac{1}{\mu^2} \mathbf{J}^T \mathbf{J} \quad (29)$$

or

$$\tilde{\mathbf{R}}^T \tilde{\mathbf{R}} = \frac{1}{\mu^2} \mathbf{J}^T \mathbf{J} \quad (30)$$

Let $\mathbf{J} = \mathbf{Q}\mathbf{R}$, where \mathbf{R} is an $n \times n$ upper-triangular matrix with positive diagonal entries and \mathbf{Q} is an $n \times n$ real unitary matrix. Then, eq. (30) can be simplified as

$$\tilde{\mathbf{R}}^T \tilde{\mathbf{R}} = \frac{1}{\mu^2} \mathbf{R}^T \mathbf{R} \quad (31)$$

Since both sides of eq. (31) are in the form of Cholesky factorization for the positive definite symmetric matrix $\mathbf{J}^T \mathbf{J}$ (Golub and Van Loan, 1983), we conclude

$$\tilde{\mathbf{R}} = \frac{1}{\mu} \mathbf{R} \quad (32)$$

Substituting eq. (27) into eq. (15), we obtain

$$\tilde{\mathbf{R}}^T \tilde{\mathbf{Q}}^T \cdot [1, 1, \dots, 1]^T = \underline{0} \quad (33)$$

Since $\tilde{\mathbf{R}}$ is non-singular and its null space is zero, we conclude

$$\tilde{\mathbf{Q}}^T \cdot [1, 1, \dots, 1]^T = \underline{0} \quad (34)$$

Since $\tilde{\mathbf{Q}}$ is a unitary matrix, we have

$$\tilde{\mathbf{Q}}^T \tilde{\mathbf{Q}} = \mathbf{I}_n \quad (35)$$

Let \mathbf{A}_i be the matrix given by eq. (26); then \mathbf{A}_i satisfies eqs. (15) and (18). Comparing eqs. (34) and (35) with (15) and (18), we conclude that the upper pseudo-triangular unitary matrix $\tilde{\mathbf{Q}}$ is given by

$$\tilde{\mathbf{Q}}^T = \frac{1}{\kappa} \mathbf{A}_i^T \quad (36)$$

Substituting eqs. (32) and (36) into eq. (27), we obtain

$$\mathbf{A}^T = \frac{1}{c} \mathbf{R}^T \mathbf{A}_i^T \quad (37)$$

Equation (37) provides a mean of finding the structure matrix \mathbf{A}^T for a general manipulator to yield isotropic transmission characteristics at a specified manipulator posture.

MANIPULATORS WITH GENERAL STRUCTURE MATRICES

In this section, the synthesis of structure matrices of the general form will be discussed. For a general structure matrix, $\tilde{\mathbf{Q}}$ in eq. (27) takes the form of a general unitary matrix. Following the procedure outlined from eq. (27) to (35), it can be shown that a general unitary matrix $\tilde{\mathbf{Q}}$ satisfying eqs. (34) and (35) is given by

$$\tilde{\mathbf{Q}}^T = \frac{1}{\kappa} \mathbf{U}^T \mathbf{A}_i^T \quad (38)$$

where \mathbf{U} is an arbitrary real $n \times n$ unitary matrix. Substituting eqs. (32)

and (38) into (27) and taking its transpose, yields

$$\mathbf{A}^T = \frac{1}{c} \mathbf{R}^T \mathbf{U}^T \mathbf{A}_i^T \quad (39)$$

or

$$\mathbf{A}^T = \frac{1}{c} \mathbf{J}^T \tilde{\mathbf{U}}^T \mathbf{A}_i^T \quad (40)$$

where $\tilde{\mathbf{U}} = \mathbf{U}\mathbf{Q}^T$ is also a real unitary matrix.

Note that the matrix \mathbf{A}^T obtained by using eq. (39) or (40) may not necessarily satisfy condition C3, that is non-zero elements in the columns of \mathbf{A}^T may not necessarily be consecutive.

If isotropic transmission is to be achieved at the special manipulator posture, where the condition number of the Jacobian matrix \mathbf{J} is equal to one, then eq. (39) or (40) can be reduced to the following form:

$$\mathbf{A}^T = \frac{1}{c} \mathbf{U}^T \mathbf{A}_i^T \quad (41)$$

Equations (39), (40), and (41) provide a method for generating a general structure matrix with isotropic transmission characteristics.

As mentioned earlier, the Jacobian matrix of a manipulator is position dependent. Therefore, the condition number of matrix $\mathbf{A}^{+T} \mathbf{J}^T$ will change as the end-effector moves away from the reference posture. In what follows, we prove that the condition number of a general isotropic structure matrix follows that of the pseudo-triangular isotropic structure matrix.

Substituting eq. (39) into the matrix $\mathbf{A}^{+T} \mathbf{J}^T$ and simplifying it, we

obtain

$$\mathbf{A}^{+T} \mathbf{J}^T = (\frac{1}{c} \mathbf{A}_i \tilde{\mathbf{U}} \mathbf{R})^{+T} \mathbf{J}^T = \frac{1}{c\mu^2} \mathbf{A}_i \tilde{\mathbf{U}} \mathbf{R} (\mathbf{R}^T \mathbf{R})^{-1} \mathbf{J}^T \quad (42)$$

Since multiplying a real unitary matrix to a matrix does not change the condition number of the matrix, we can write

$$\begin{aligned} \text{cond}(\mathbf{A}^{+T} \mathbf{J}^T) &= \text{cond}(\frac{1}{c\mu^2} \mathbf{A}_i \tilde{\mathbf{U}} \mathbf{R} (\mathbf{R}^T \mathbf{R})^{-1} \mathbf{J}^T) = \\ \text{cond}(\frac{1}{c\mu^2} \mathbf{A}_i \mathbf{R} (\mathbf{R}^T \mathbf{R})^{-1} \mathbf{J}^T) &= \text{cond}((\frac{1}{c} \mathbf{A}_i \mathbf{R})^{+T} \mathbf{J}^T) \end{aligned} \quad (43)$$

where $\text{cond}()$ denotes the condition number of the matrix in the parenthesis. Equation (43) states that the two matrices, $\mathbf{A}^{+T} \mathbf{J}^T$ and $(\mathbf{A}_i \mathbf{R})^{+T} \mathbf{J}^T$, share the same condition number. We conclude that if two manipulators, one has a structure matrix of the general form while the other has a pseudo-triangular matrix, are designed to possess isotropic transmission characteristics at the same manipulator posture, then the two manipulators will have identical condition numbers everywhere within their workspaces.

EXAMPLES

Example 1: Two-dof Manipulator

A two-dof planar manipulator, with its link lengths proportional to $1/\sqrt{2} : 1$ as shown in Fig. 3, is selected for the purpose of demonstration. The Jacobian matrix for this manipulator is given by

$$\mathbf{J} = \ell \begin{bmatrix} -S_{12}/\sqrt{2} & -S_2 - S_{12}/\sqrt{2} \\ C_{12}/\sqrt{2} & C_2 + C_{12}/\sqrt{2} \end{bmatrix} \quad (44)$$

where $C_2 = \text{Cos}(\theta_2)$, $S_2 = \text{Sin}(\theta_2)$, $C_{12} = \text{Cos}(\theta_1 + \theta_2)$, $S_{12} = \text{Sin}(\theta_1 + \theta_2)$ and

ℓ is the second link length. Note that the link lengths has been proportioned in such a way that its Jacobian matrix, \mathbf{J} , has a unity condition number when the manipulator assumes the $\theta_1 = 225^\circ$ posture. Also note that the links and joints are numbered from the distal end.

Three different 2×3 pseudo-triangular structure matrices as shown in Table 1 are synthesized for the purpose of comparison. All three structures matrices share the same tendon routing as shown in Fig. 4. However, their pulley sizes are different from one another. Structure (a) is a structure matrix derived from eq. (26). Hence, structure (a) will possess isotropic transmission characteristics when its end-effector is positioned at $x = \ell/\sqrt{2}$, and $y = 0$. Structure (b) uses equal size pulleys. It does not possess isotropic transmission characteristics. Structure (c) is calculated from eq. (37) based on the condition that the manipulator will possess isotropic transmission characteristics when the end-effector is positioned at the $x = \ell$, $y = 0$. At $x = \ell$ and $y = 0$, the Jacobian matrix becomes

$$\mathbf{J} = \begin{bmatrix} 0.6614 & 0 \\ 0.2500 & 1 \end{bmatrix} \quad (45)$$

Using QR factorization, we obtain

$$\mathbf{Q} = \begin{bmatrix} 0.9354 & -0.3536 \\ 0.3536 & 0.9354 \end{bmatrix} \quad and \quad \mathbf{R} = \begin{bmatrix} 0.7071 & 0.3536 \\ 0 & 0.9354 \end{bmatrix} \quad (46)$$

where \mathbf{R} is calculated so that its diagonal terms are both positive. Substituting \mathbf{R} from eq. (46) and the structure matrix (a) from Table 1 into eq. (37) and after rescaling, yields the structure matrix (c) as shown in Table 1. The homogeneous solutions and the condition numbers of the structure matrices, \mathbf{A}^T , are also listed in Table 1. We note that the null

vectors of structures (a) and (c) both point in the isotropic direction.

For these two-dof systems, if we confine the externally applied force, \underline{f} , to be bounded on a unit circle, then the particular solution ξ_p lies on an ellipse as shown in Fig. 5. To achieve a fair comparison, the values of κ in Table 1 are chosen so that the areas bounded by the ellipses in ξ_p -space are all equal to π .

Figure 6 shows the variation of condition numbers of $\mathbf{A}^{+T}\mathbf{J}^T$ as functions of the end-effector position. Structure (a) has a unity condition number at the $x = \ell/\sqrt{2}$ and $y = 0$ (or $\theta_1 = 225^\circ$) position. The condition number of structure (b) is fairly close to that of structure (a) due to the fact that the two structure matrices differ from each other by a small amount. Structure (c) has a unity condition number at the $x = \ell$ and $y = 0$ (or $\theta_1 = 249.3^\circ$) position. Comparing structure (a) with (c), structure (c) seems to be better than structure (a).

Two manipulator postures are chosen for evaluation. Position 1 is at $x = \ell$, $y = 0$, and position 2 is at $x = \ell/\sqrt{2}$, $y = 0$. Let a unity force \underline{f} be applied at the end-effector as shown in Fig. 3. Using eq. (8), the required tensions for each structure are calculated for every given direction, ϕ , of the applied force. For the purpose of comparison, we adjust the value of λ in eq. (8) such that one of the tendons will have zero tension while the other two have nonnegative tensions. As ϕ varies from 0 to 2π , each tendon force forms a closed curve.

Figures 7, 8, and 9 are polar plots of the three tendon forces for transmission structures (a), (b), and (c), respectively. In a polar plot, the

radial distance represents the magnitude of tendon force while the phase angle represents the direction of applied force. From Fig. 7-2, we note that the shapes of the three tendon forces are identical except for a shift in the phase angle. When the external force is applied along the $\phi = 30^\circ$, 150° and 270° directions, only one tendon is under tension. Under these situations, the resultant torques produced by one tendon is sufficient to work against the external force. We call these directions the “solo directions.” At any other directions, other than the solo directions, only one tendon will have zero tension. Since structure (a) is designed to possess isotropic transmission characteristics at the second position, the distribution of tensions becomes distorted as the end-effector moves to position 1 as shown in Fig. 7-1. The corresponding solo directions as shown in Fig. 7-1 also change their locations and they become unevenly spaced.

Although the condition number of structure (b) is fairly close to that of structure (a), tension distribution of structure (b) is quite different from that of structure (a) as shown in Fig. 8. We note that tension exerted on the third tendon is much larger than that on the other two. This is due to the fact that its null vector, $[1, 1, 2]^T$, points away from the isotropic direction. Structure (c) has isotropic transmission characteristics at position 1 as shown in Fig. 9-1. Again, at the isotropic point, position 1, the solo directions are evenly spaced. Both structures (a) and (c) are equally good in tension distribution. The only difference seems to be that structure (c) has higher tendon forces than that of structure (a). However, this difference can be corrected by adjusting the value of κ , i.e. the pulley sizes.

Table 2 lists the maximum value of each tendon force plotted in Figs. 7 to 9 and their ratios. The corresponding condition numbers of $\mathbf{A}^{+T} \mathbf{J}^T$ for the

manipulator at the two specified positions are also listed. It can be seen that structure (c) has the best distribution of tensions. It has a nearly 1 : 1 : 1 maximum tendon force ratios between positions 1 and 2.

Example 2: Three-dof Manipulator

A spatial three-dof manipulator as shown in Fig. 10 is used to compare the effect of different transmission structures. The joint axes are arranged such that, starting from the distal joint (first joint), the second joint axis is parallel to the first while the third is perpendicular to the second. The link lengths are proportional to $1/\sqrt{2} : 1 : 1/\sqrt{2}$. To compare the influence of different pulley sizes, the same tendon routing as shown in Fig. 11 is adapted. A unity force acting on the end-effector as shown in Fig. 10 is assumed, where ϕ is the angle the external force made with the z-axis and ψ is the angle the projected vector of the external force in x-y plane made with the x-axis. The unity force can be expressed as

$$\underline{f} = [\sin(\phi)\cos(\psi), \sin(\phi)\sin(\psi), \cos(\phi)]^T \quad (47)$$

where ϕ varies from 0 to π and ψ varies from 0 to 2π . By letting $\theta_3 = 90^\circ$, without loosing generality, the Jacobian matrix for the manipulator shown in Fig. 10 is given by

$$\mathbf{J} = \ell \begin{bmatrix} 0 & 0 & C_2 + (1 + C_{12})/\sqrt{2} \\ -S_{12}/\sqrt{2} & -S_2 - S_{12}/\sqrt{2} & 0 \\ C_{12}/\sqrt{2} & C_2 + C_{12}/\sqrt{2} & 0 \end{bmatrix} \quad (48)$$

where $C_2 = \cos(\theta_2)$, $S_2 = \sin(\theta_2)$, $C_{12} = \cos(\theta_1 + \theta_2)$, $S_{12} = \sin(\theta_1 + \theta_2)$, and ℓ is the length of the second link. For this manipulator, it can be shown that the condition number of the Jacobian matrix is equal to one when

$\theta_1=135^\circ$ and $\theta_2=45^\circ$, and that $(x = 0, y = z = \ell/\sqrt{2})$ is one such point on the locus.

Table 3 lists two different transmission structures, their corresponding homogeneous solutions, and the condition number of \mathbf{A}^T . Structure (a) has its null vector pointed in the isotropic direction. Structure (b) has its null vector pointed 31.4° away from the isotropic direction. Structure (a) is a transmission structure derived from eq. (26) while structure (b) is designed with equal size pulleys. Similar to that of two-dof manipulator, with \underline{f} bounded on a unit sphere, the values of κ in Table 3 are calculated by equating the volume enclosed by $\underline{\xi}_p$ in the particular solution space to $4\pi/3$. Two positions are chosen for evaluation. At position 1: $x = 0, y = z = \ell/\sqrt{2}$, and at position 2: $x = 0, y = \ell + \ell/\sqrt{2}, z = 0$.

Figures 12-1 through 12-4 show the spherical plots of tensions in tendons 1, 2, 3, and 4, respectively, of structure (a) with the end-effector located at position 1. In a spherical plot, the radial distance represents the tension, and the direction represents the direction of applied force. Since position 1 is an isotropic point for structure (a), the four figures are identical in shape with one another, i.e. Figs. 12-2 through 12-4 will look like Fig. 12-1 when they are viewed from some appropriate angles. The solo directions for the four tendons are evenly distributed, and are given by $(\phi=35.3^\circ, \psi=305.3^\circ)$, $(\phi=144.7^\circ, \psi=305.3^\circ)$, $(\phi=90^\circ, \psi=70.5^\circ)$, and $(\phi=90^\circ, \psi=180^\circ)$, respectively. The separation angle between every two solo directions is 109.5° . Figures (13-1)-(13-4) are the corresponding spherical plots of tensions for structure (b) when the end-effector is located at position 1. Note that these four figures are different from one another since structure (b) doesn't possess isotropic transmission characteristics. Figures (14-1)-(14-

4) and (15-1)-(15-4) are the spherical plots of tensions for structures (a) and (b), respectively, when the end-effector is located at position 2. Table 4 lists the maximum tensions, their ratios, and the condition numbers of $\mathbf{A}^{+T}\mathbf{J}^T$ of the manipulator at the two specified positions.

The overall condition number depends on kinematic structure and transmission structure of a manipulator. It is strongly position dependent. Yet, it can be seen from Table 4 that, even the condition number of structure (a) is worse than that of structure (b) at position 2, structure (a) still has better maximum tension ratios than that of structure (b), i.e. 1.034 : 1 : 1.051 : 1.051 as compared with 1 : 1 : 1.992 : 3.714. Also the largest maximum tension in structure (a) is far less than that of structure (b). This is because the null vector of structure (a) points in the isotropic direction while that of structure (b) points in the $[1, 1, 2, 4]^T$ direction.

CONCLUSIONS

A methodology for the kinematic synthesis of tendon-driven manipulators has been developed. Design equations for synthesizing a manipulator with isotropic transmission characteristics at a given manipulator posture are derived. These equations are then applied to two different types of kinematic structures. The first type has pseudo-triangular structure matrices and the second type has structure matrices of the general form. The structure matrices of the first type can be obtained by post-multiplying the isotropic structure matrix, \mathbf{A}_i , by the \mathbf{R} matrix, where \mathbf{R} is obtained by performing a QR factorization of the Jacobian matrix. Structure matrices of the second type can be derived by post-multiplying \mathbf{A}_i by \mathbf{UR} ,

where \mathbf{U} is an arbitrary unitary matrix. Two examples, one two-dof planar manipulator and one three-dof spatial manipulator, are used to demonstrate the methodology. It is shown that manipulators which possess isotropic transmission characteristics do have more even force distribution among their tendons. It is also shown that the direction of homogeneous solution plays a very important role in tendon force distribution.

ACKNOWLEDGMENT

This work was supported in part by the U.S. Department of Energy under Grant DEF05-88ER13977, and in part by the NSF Engineering Research Centers Program NSFD CDR 8803012. Such support does not constitute an endorsement by the supporting agencies of the views expressed in the paper.

REFERENCES

Asada, H. and Cro Granito, J. A., 1985, "Kinematic and Static Characterization of Wrist Joints and Their Optimal Design," *Proc. of IEEE Int'l. Conf. on Robotics and Automation*, pp. 244-250.

Ben-Israel, A. and Greville, T. N. E., 1974, "*Generalized Inverses: Theory and Applications.*" Wiley, New York.

Chen, D. Z. and Tsai, L. W., 1990, "Kinematic and Dynamic Synthesis

of Geared Robotic Mechanisms,” ASME DE-Vol. 26, Cams, Gears, Robot and Mechanism Design, pp. 397-404.

Golub, G. H. and Van Loan, C. F., 1983 “*Matrix Computations.*” The John Hopkins University Press, Baltimore, Maryland.

Gosselin, C. and Angeles, J., 1988, “A New Performance Index for the Kinematic Optimization of Robotic Manipulators,” ASME Trends and Developments in Mechanisms, Machines and Robotics, DE-Vol. 15-3, pp. 441-447.

Jacobsen, S. C., Wood, J. E., Knutti, D. F., and Biggers, K. B., 1985, “The Utah/MIT Dexterous Hand: Work in Progress,” The Int’l. J. of Robotics Research, Vol. 3, No. 4, pp. 21-50.

Lee, J. J. and Tsai, L. W., 1991, “On the Structural Synthesis of Tendon-Driven Manipulators Having Pseudo-Triangular Matrix,” The Int’l. J. of Robotics Research, Vol. 10, No. 3., pp. 255-262.

Lee, J. J., 1991, “Tendon-Driven Manipulators: Analysis, Synthesis, and Control,” Ph.D. Dissertation, Dept. of Mech. Eng., The University of Maryland, College Park, MD.

Morecki, A., Busko, Z., Gasztold, H., and Jaworek, K., 1980, “Synthesis and Control of the Anthropomorphic Two-Handed Manipulator,” *Proc. 10th Int’l. Symposium on Industrial Robots*, Milan, Italy, pp. 461-474.

Okada, T., 1977, “On a Versatile Finger System,” *Proc. 7th Int’l.*

Symposium on Industrial Robots, Tokyo, Japan, pp. 345-352.

Rovetta, A., 1977, "On Specific Problems of Design of Multipurpose of Mechanical Hands in Industrial Robots," *Proc. 7th Int'l. Symposium on Industrial Robots*, Tokyo, Japan, pp. 337-341.

Salisbury, J. K. and Craig, J. J., 1982, "Articulated Hands: Force Control and Kinematic Issues," *The Int'l. J. of Robotics Research*, Vol. 1, No. 1, pp. 4-17.

Salisbury, J. K., 1982, "Kinematic and Force Analysis of Articulated Hands," Ph.D. Dissertation, Mech. Eng. Dept., Stanford University, Stanford, CA.

Strang, G., 1980, "*Linear Algebra and Its Applications*," 2nd ed., Academic Press, New York.

Sugano, S. and Kato, I., 1987, "WABOT-2: Autonomous Robot with Dexterous Finger-Arm," *Proc. of IEEE Int'l. Conf. on Robotics and Automation*, Raleigh, North Carolina, pp. 90-97.

Yoshikawa, T., 1985, "Manipulability of Robotic Mechanisms," *Int'l. J. of Robotics Research*, Vol. 4, No. 2, pp. 3-9.

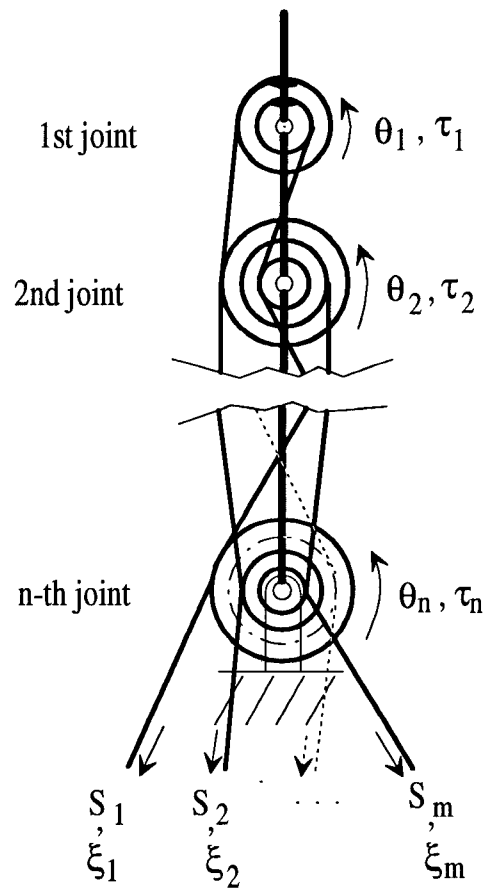


Fig. 1 Planar schematic of an n -dof tendon-driven manipulator

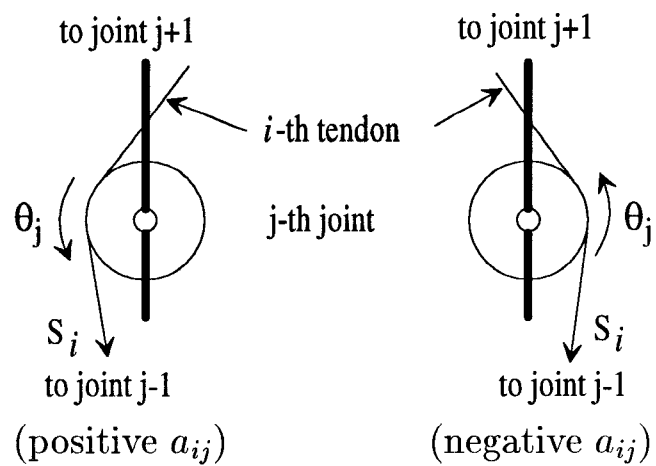


Fig. 2 Sign convention for a_{ij}

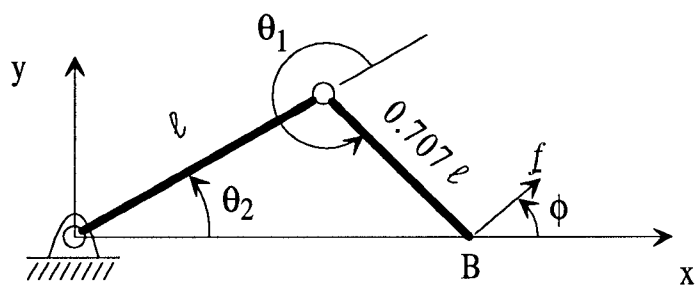


Fig. 3 Two-dof planar manipulator

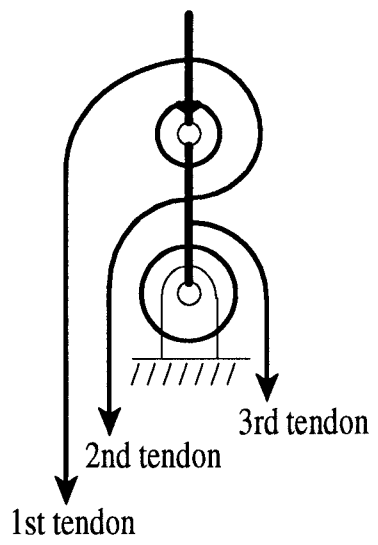


Fig. 4 Tendon routing in two-dof manipulator

Transmission Structure	\mathbf{A}^T	κ	$\underline{\xi}_h$	$\text{Cond}(\mathbf{A}^T)$
a	$\kappa \begin{bmatrix} 1 & -1 & 0 \\ \frac{1}{\sqrt{3}} & \frac{1}{\sqrt{3}} & \frac{-2}{\sqrt{3}} \end{bmatrix}$	0.500	$\begin{bmatrix} 1 \\ 1 \\ 1 \end{bmatrix}$	1
b	$\kappa \begin{bmatrix} 1 & -1 & 0 \\ 1 & 1 & -1 \end{bmatrix}$	0.4082	$\begin{bmatrix} 1 \\ 1 \\ 2 \end{bmatrix}$	1.2247
c	$\kappa \begin{bmatrix} 1 & -1 & 0 \\ 1.2638 & 0.2637 & -1.5275 \end{bmatrix}$	0.3780	$\begin{bmatrix} 1 \\ 1 \\ 1 \end{bmatrix}$	1.6684

Table 1: Three transmission structures and their kinematic properties

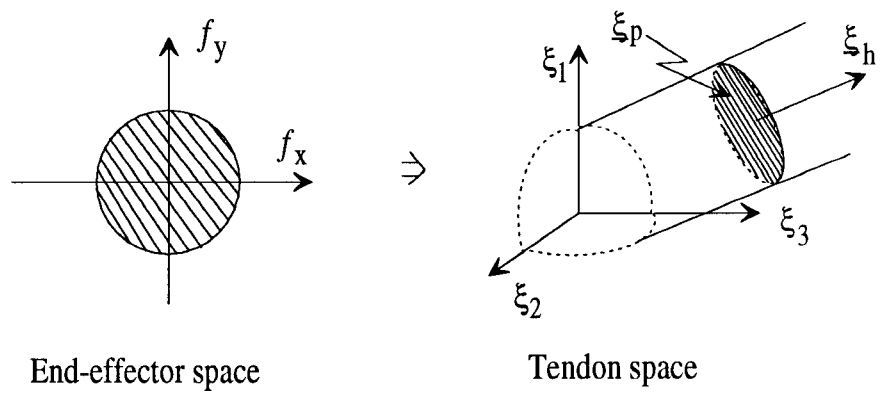


Fig. 5 Space relationship for a two-dof tendon-driven manipulator

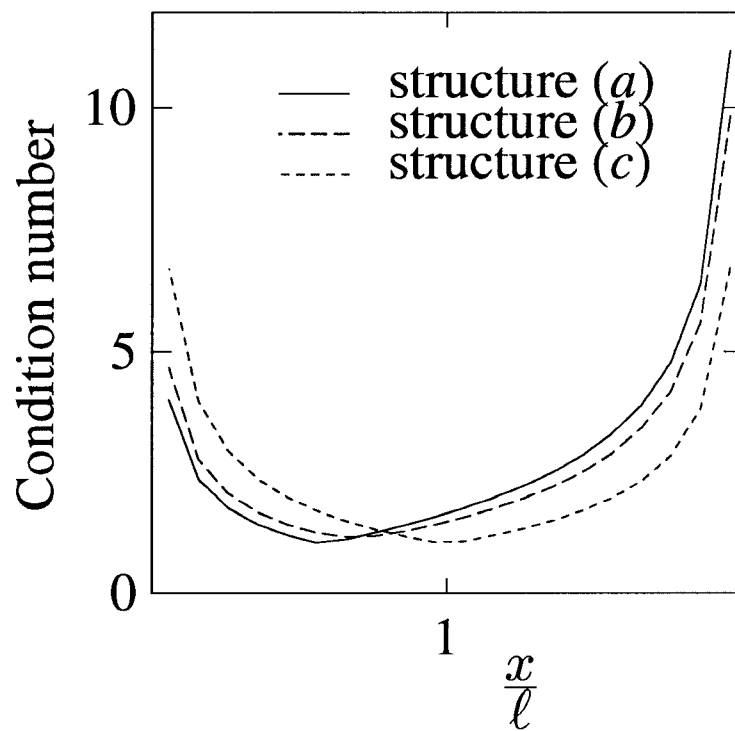


Fig. 6 Condition number of four transmission structures

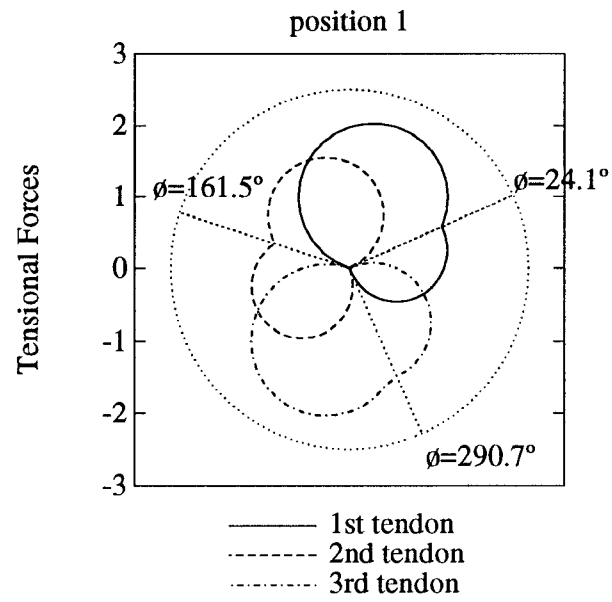


Fig. 7-1 Tension distribution in transmission structure (a), evaluated at position 1

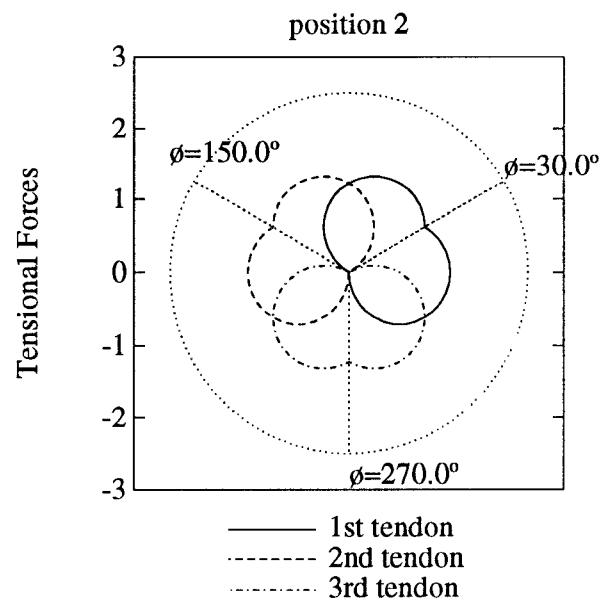


Fig. 7-2 Tension distribution in transmission structure (a), evaluated at position 2

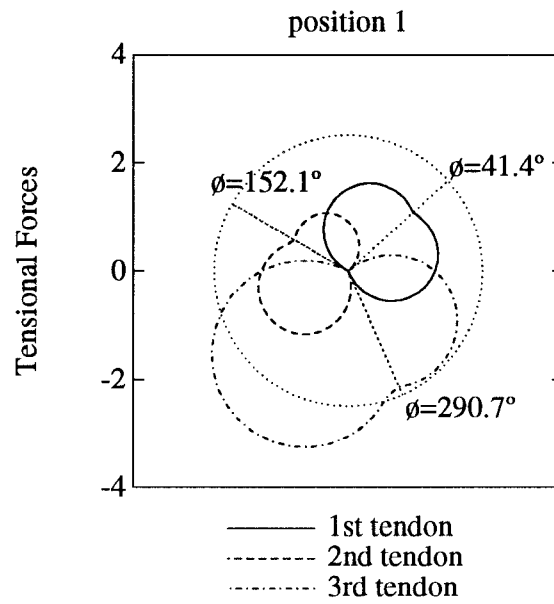


Fig. 8-1 Tension distribution in transmission structure (*b*), evaluated at position 1

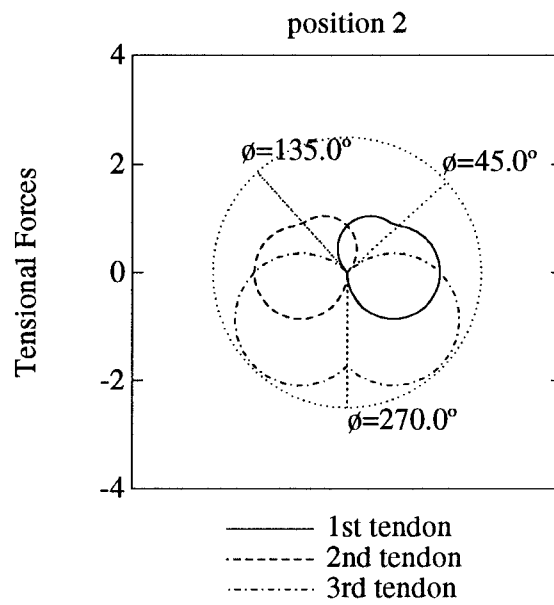


Fig. 8-2 Tension distribution in transmission structure (*b*), evaluated at position 2

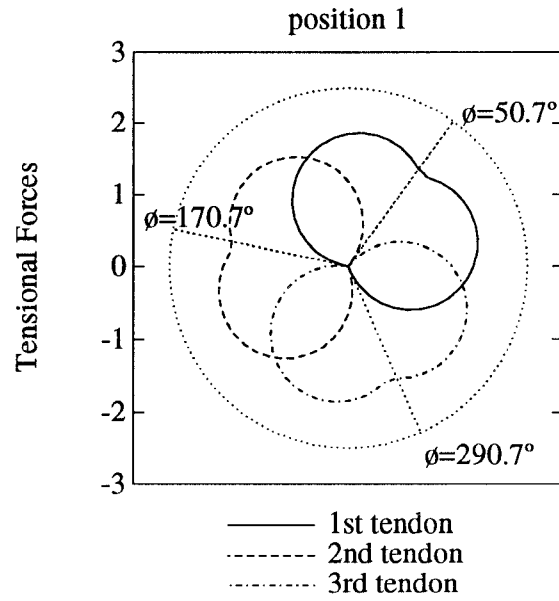


Fig. 9-1 Tension distribution in transmission structure (c), evaluated at position 1

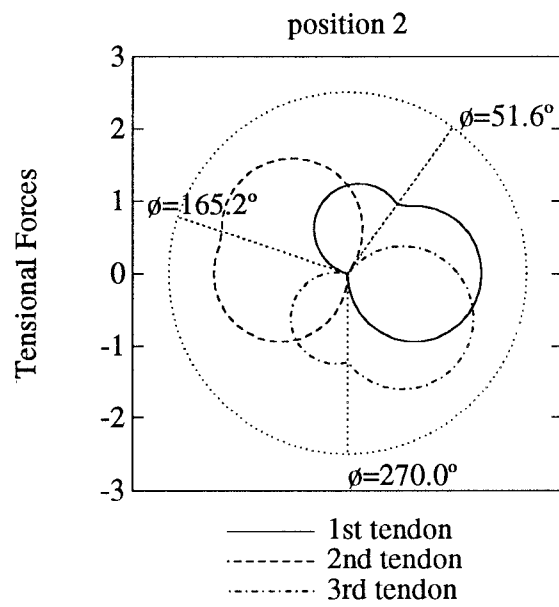


Fig. 9-2 Tension distribution in transmission structure (c), evaluated at position 2

Structure		a	b	c
position 1	max. tensions	$\begin{bmatrix} 2.089 \\ 1.623 \\ 2.089 \end{bmatrix}$	$\begin{bmatrix} 1.731 \\ 1.731 \\ 3.462 \end{bmatrix}$	$\begin{bmatrix} 1.869 \\ 1.869 \\ 1.869 \end{bmatrix}$
	ratio	1.287:1:1.287	1:1:2.001	1:1:1
	Cond($\mathbf{A}^{+T}\mathbf{J}^T$)	1.6684	1.4884	1
position 2	max. tensions	$\begin{bmatrix} 1.414 \\ 1.414 \\ 1.414 \end{bmatrix}$	$\begin{bmatrix} 1.732 \\ 1.732 \\ 2.446 \end{bmatrix}$	$\begin{bmatrix} 1.871 \\ 1.972 \\ 1.972 \end{bmatrix}$
	ratio	1:1:1	1:1:1.412	1:1.054:1.054
	Cond($\mathbf{A}^{+T}\mathbf{J}^T$)	1	1.2247	1.6684

Table 2: List of max. tensions, corresponding ratio and condition number

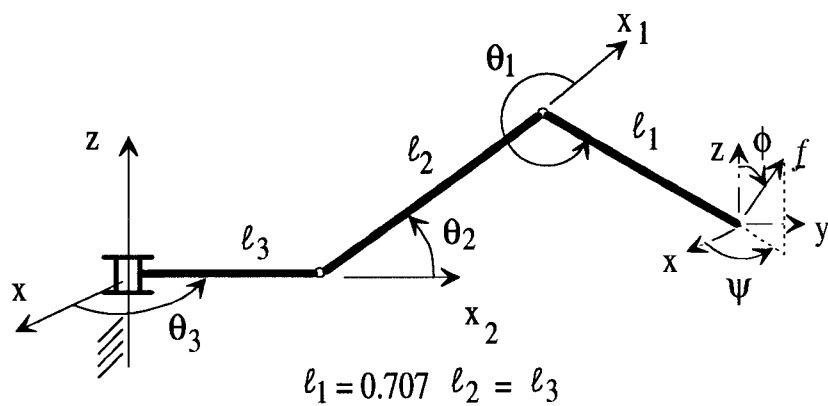


Fig. 10 Three-dof manipulator and external force \underline{f}

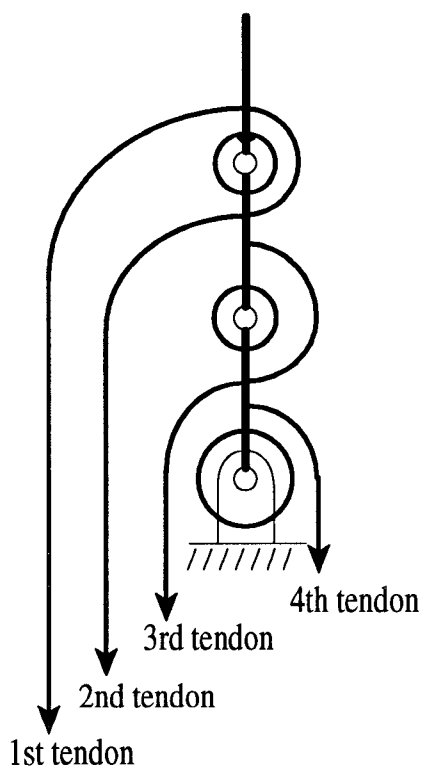
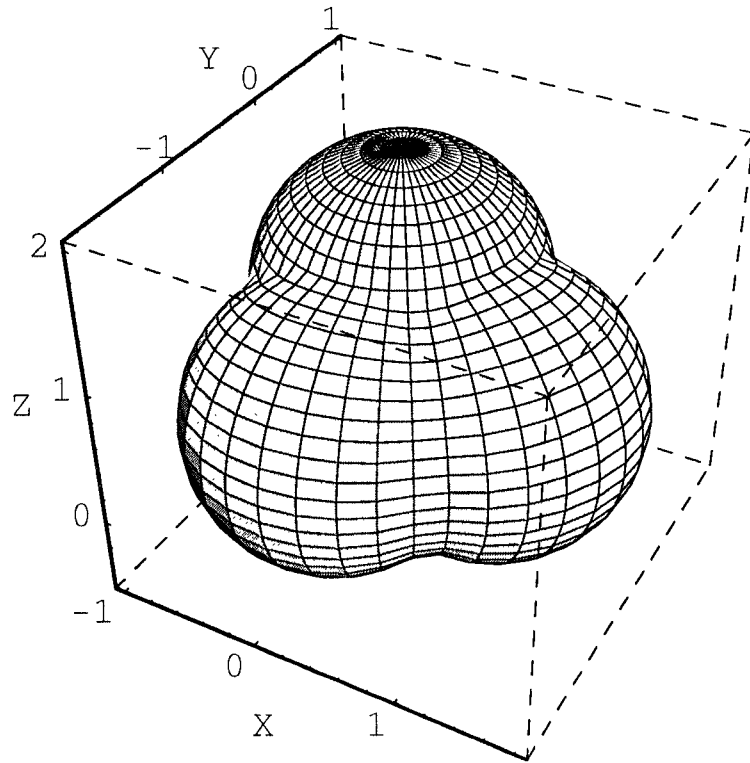


Fig. 11 Tendon routing in three-dof manipulator

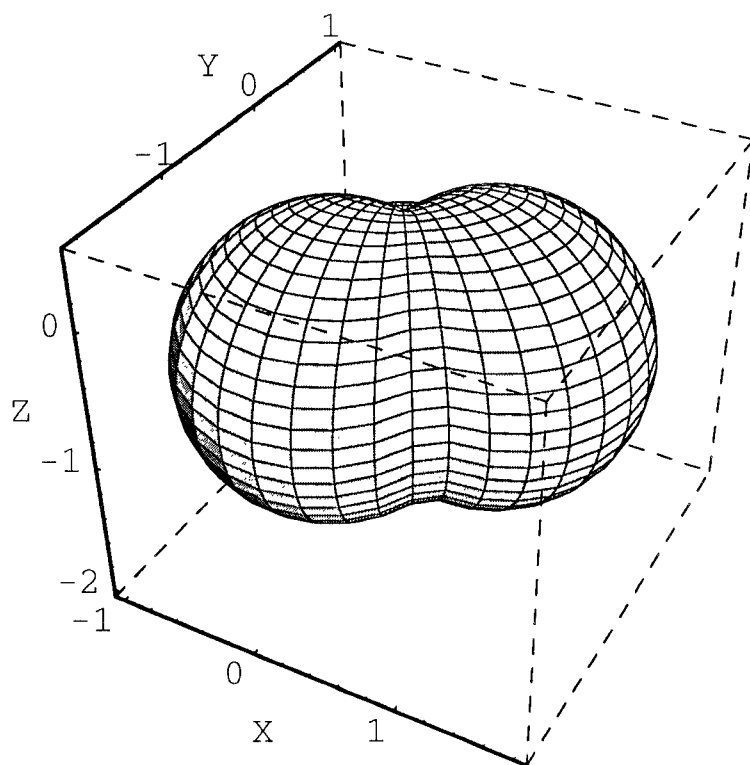
Transmission Structure	\mathbf{A}^T	κ	$\underline{\xi}_h$	$\text{Cond}(\mathbf{A}^T)$
a	$\kappa \begin{bmatrix} 1 & -1 & 0 & 0 \\ \frac{1}{\sqrt{3}} & \frac{1}{\sqrt{3}} & \frac{-2}{\sqrt{3}} & 0 \\ \frac{1}{\sqrt{6}} & \frac{1}{\sqrt{6}} & \frac{1}{\sqrt{6}} & \frac{-2}{\sqrt{6}} \end{bmatrix}$	0.3536	$\begin{bmatrix} 1 \\ 1 \\ 1 \\ 1 \end{bmatrix}$	1
b	$\kappa \begin{bmatrix} 1 & -1 & 0 & 0 \\ 1 & 1 & -1 & 0 \\ 1 & 1 & 1 & -1 \end{bmatrix}$	0.2132	$\begin{bmatrix} 1 \\ 1 \\ 2 \\ 4 \end{bmatrix}$	1.5195

Table 3: Two transmission structures and their kinematic properties



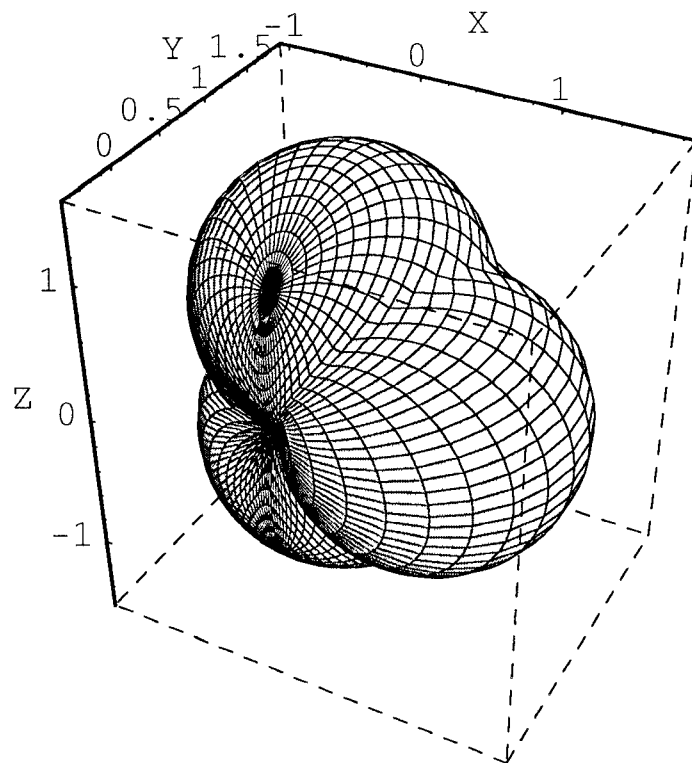
Solo direction: $\phi = 35.3^\circ$, $\psi = 305.3^\circ$

Fig. 12-1 Tension variation in tendon 1 of structure (a),
evaluated at position 1



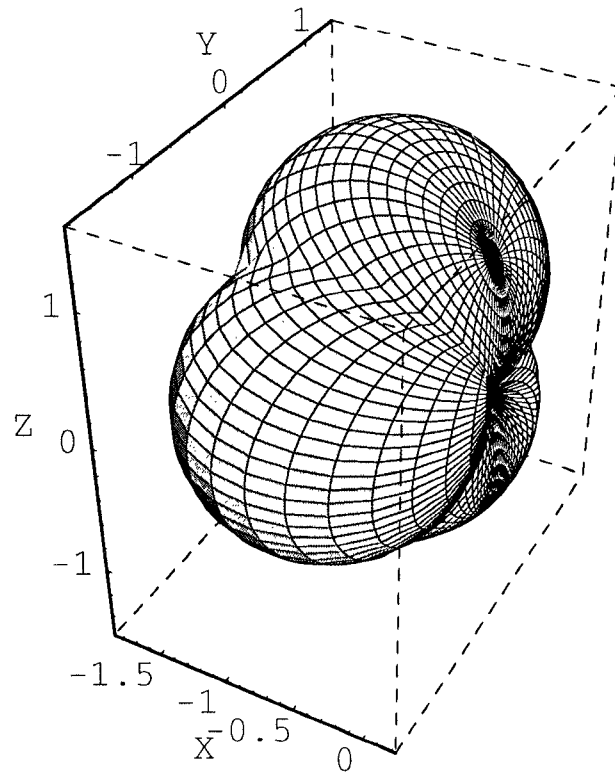
Solo direction: $\phi = 144.7^\circ$, $\psi = 305.3^\circ$

Fig. 12-2 Tension variation in tendon 2 of structure (a),
evaluated at position 1



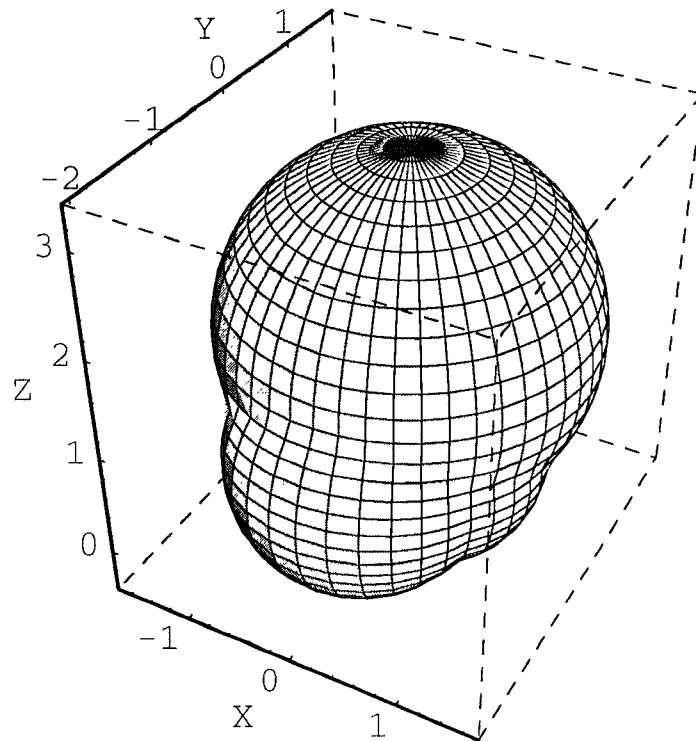
Solo direction: $\phi = 90^\circ$, $\psi = 70.5^\circ$

Fig. 12-3 Tension variation in tendon 3 of structure (a),
evaluated at position 1



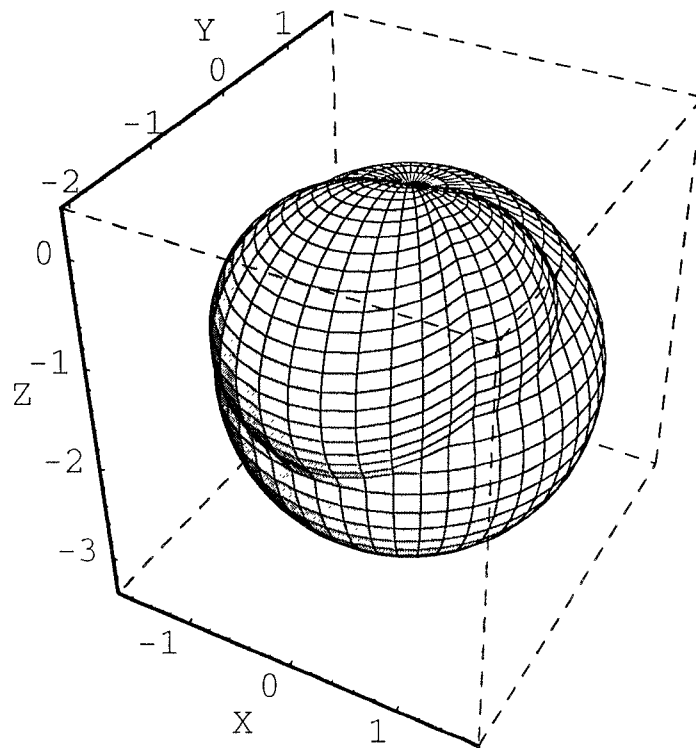
Solo direction: $\phi = 90^\circ$, $\psi = 180^\circ$

Fig. 12-4 Tension variation in tendon 4 of structure (a),
evaluated at position 1



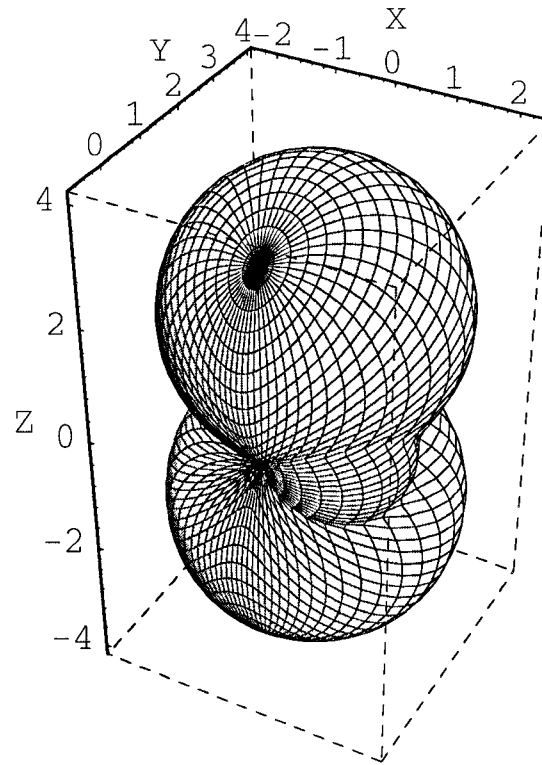
Solo direction: $\phi = 54.7^\circ$, $\psi = 315^\circ$

Fig. 13-1 Tension variation in tendon 1 of structure (b),
evaluated at position 1



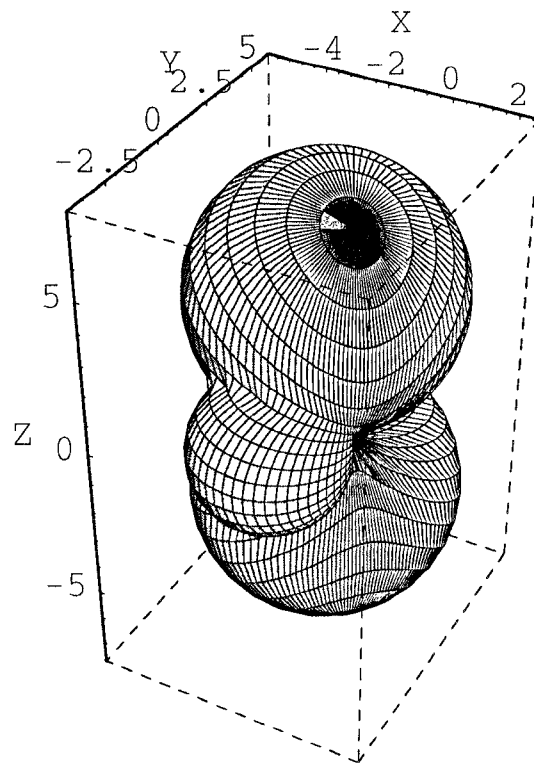
Solo direction: $\phi = 125.3^\circ$, $\psi = 315^\circ$

Fig. 13-2 Tension variation in tendon 2 of structure (b),
evaluated at position 1



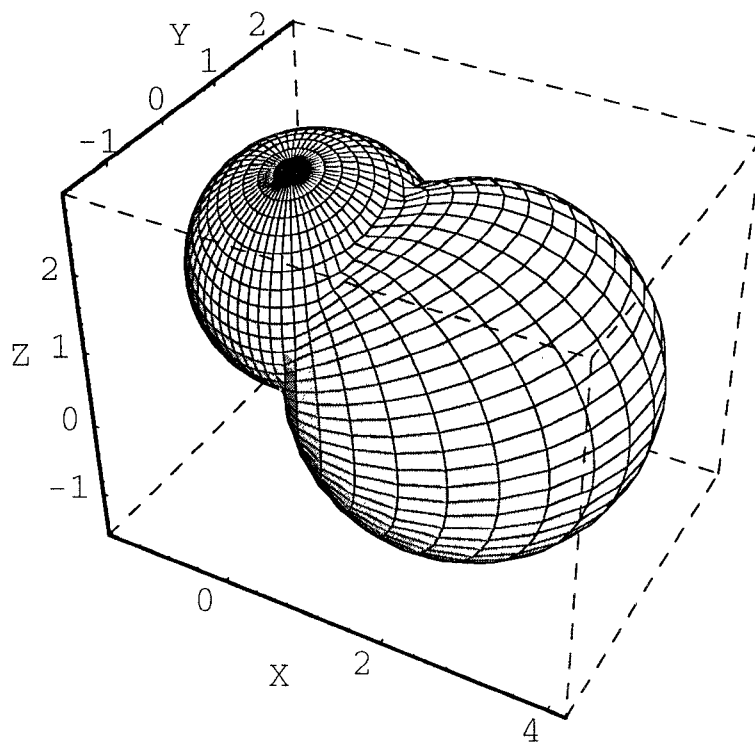
Solo direction: $\phi = 90^\circ$, $\psi = 45^\circ$

Fig. 13-3 Tension variation in tendon 3 of structure (b),
evaluated at position 1



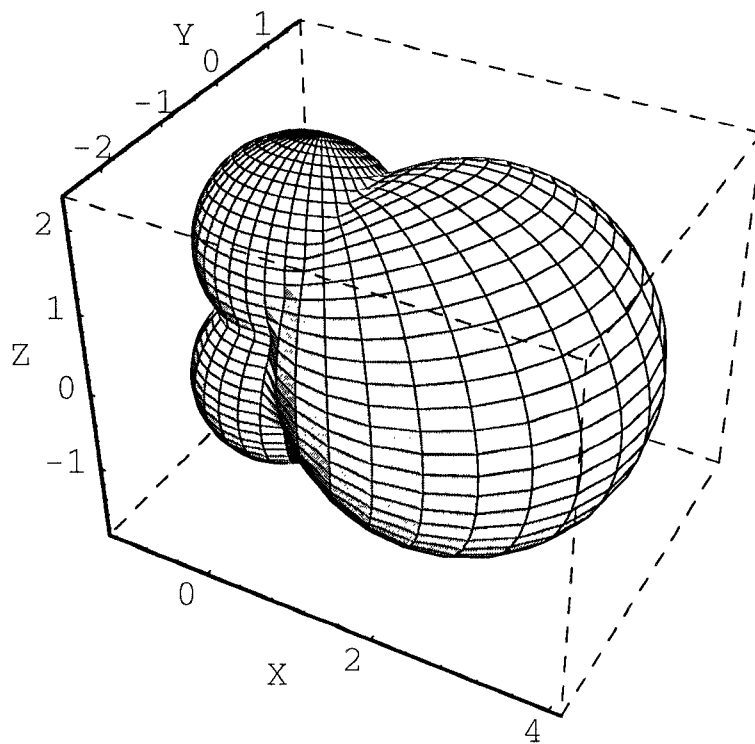
Solo direction: $\phi = 90^\circ$, $\psi = 180^\circ$

Fig. 13-4 Tension variation in tendon 4 of structure (b),
evaluated at position 1



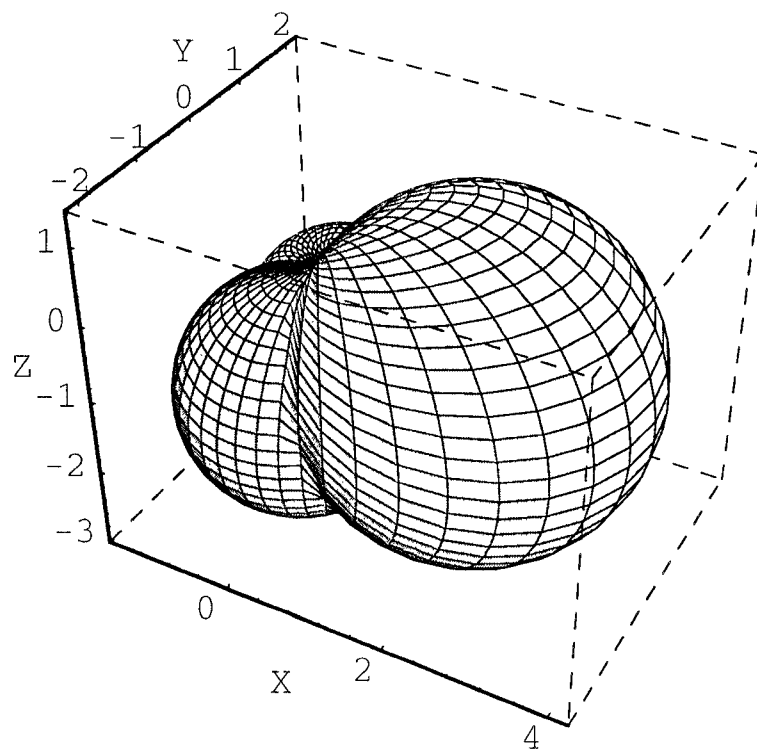
Solo direction: $\phi = 66.3^\circ$, $\psi = 79.5^\circ$

Fig. 14-1 Tension variation in tendon 1 of structure (a),
evaluated at position 2



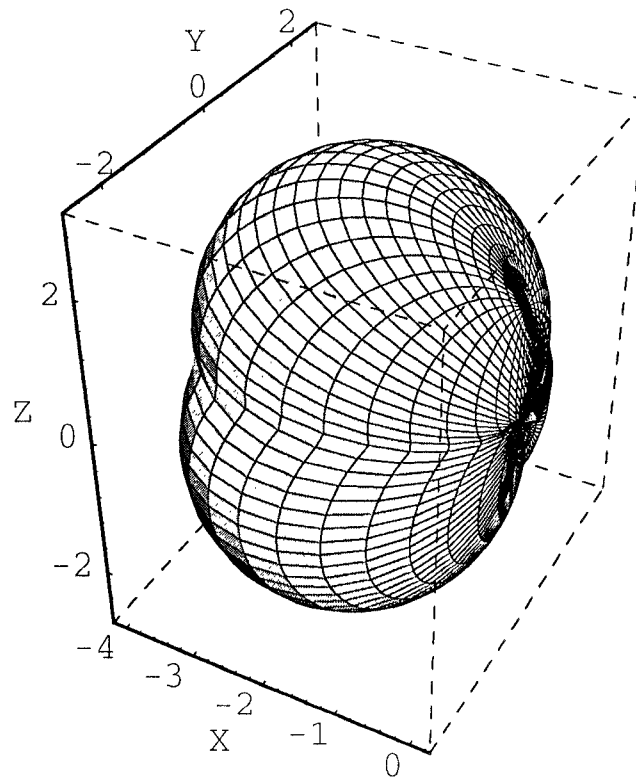
Solo direction: $\phi = 71.7^\circ$, $\psi = 277.9^\circ$

Fig. 14-2 Tension variation in tendon 2 of structure (a),
evaluated at position 2



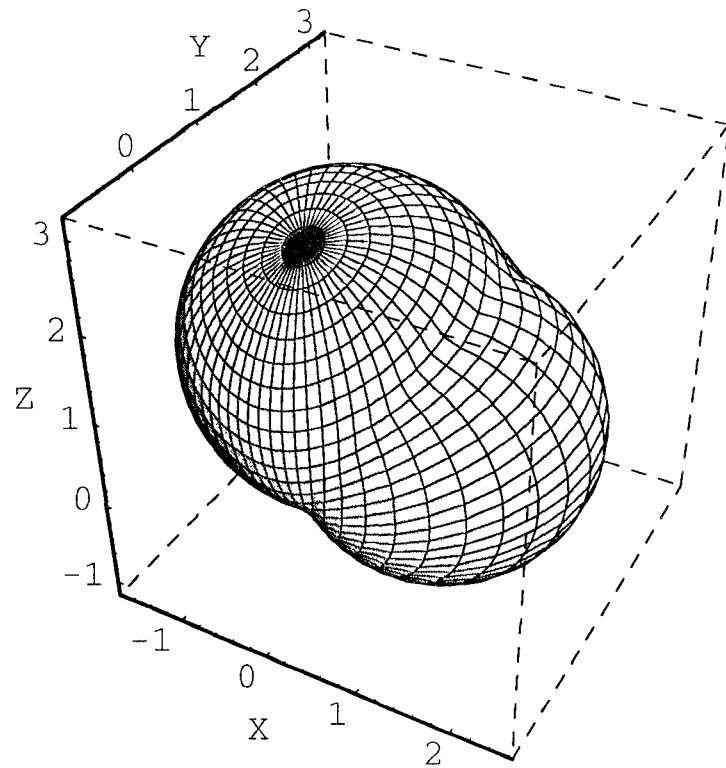
Solo direction: $\phi = 156.7^\circ$, $\psi = 61.3^\circ$

Fig. 14-3 Tension variation in tendon 3 of structure (a),
evaluated at position 2



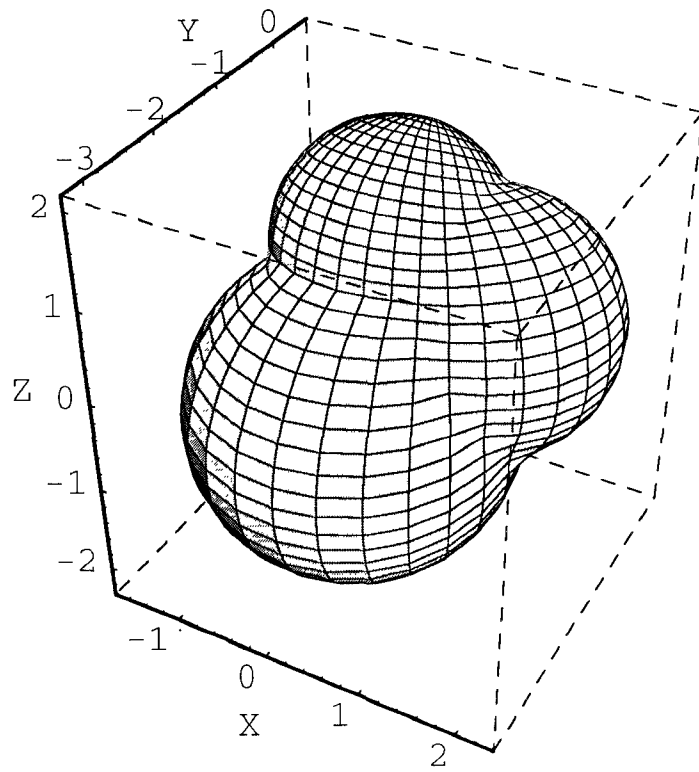
Solo direction: $\phi = 90^\circ$, $\psi = 180^\circ$

Fig. 14-4 Tension variation in tendon 4 of structure (a),
evaluated at position 2



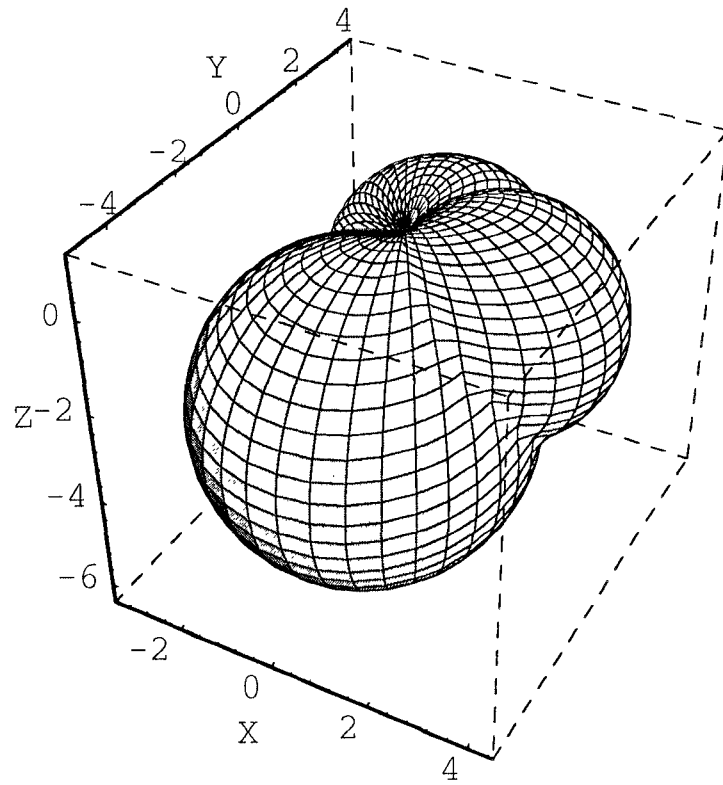
Solo direction: $\phi = 51.9^\circ$, $\psi = 62.7^\circ$

Fig. 15-1 Tension variation in tendon 1 of structure (b),
evaluated at position 2



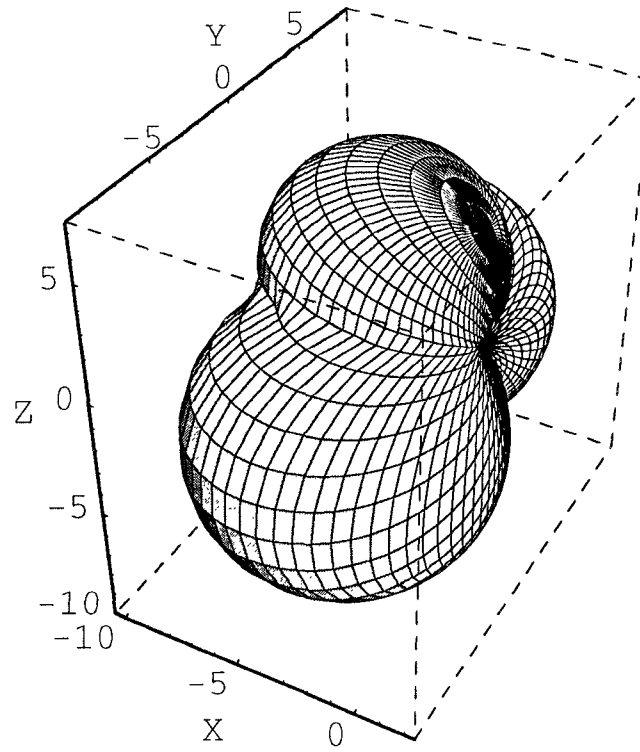
Solo direction: $\phi = 63.2^\circ$, $\psi = 287.2^\circ$

Fig. 15-2 Tension variation in tendon 2 of structure (b),
evaluated at position 2



Solo direction: $\phi = 145.1^\circ$, $\psi = 32.8^\circ$

Fig. 15-3 Tension variation in tendon 3 of structure (b),
evaluated at position 2



Solo direction: $\phi = 90^\circ, \psi = 180^\circ$

Fig. 15-4 Tension variation in tendon 4 of structure (b),
evaluated at position 2

Structure		a	b
1	position	$\begin{bmatrix} 2 \\ 2 \\ 2 \\ 2 \end{bmatrix}$	$\begin{bmatrix} 3.317 \\ 3.317 \\ 4.690 \\ 8.121 \end{bmatrix}$
	ratio	1:1:1:1	1:1:1.414:2.449
	$\text{Cond}(\mathbf{A}^{+T} \mathbf{J}^T)$	1	1.520
2	position	$\begin{bmatrix} 4.2 \\ 4.062 \\ 4.267 \\ 4.267 \end{bmatrix}$	$\begin{bmatrix} 3.315 \\ 3.315 \\ 6.604 \\ 12.310 \end{bmatrix}$
	ratio	1.034:1:1.051:1.051	1:1:1.992:3.714
	$\text{Cond}(\mathbf{A}^{+T} \mathbf{J}^T)$	2.7112	2.1727

Table 4: List of max. tensions, corresponding ratio and condition number

